CALIBRATION FOR CODA BASED MAGNITUDE AND YIELD

W. Scott Phillips, Howard J. Patton, Steven R. Taylor, Hans E. Hartse, and George E. Randall

Los Alamos National Laboratory

Sponsored by National Nuclear Security Administration
Office of Nonproliferation Research and Engineering
Office of Defense Nuclear Nonproliferation

Contract No. W-7405-ENG-36

ABSTRACT

The stability of local (<100 km) earthquake coda has been well established through observations that have shown coda amplitudes to be independent of distance, path details, and azimuth with respect to the focal mechanism. This behavior is consistent with scattered energy models of coda and allows accurate measurement of relative amplitudes. Furthermore, relative coda amplitudes can be measured to a high precision because of the redundant information in adjacent time windows. These properties have been employed to produce absolute source spectra from the relative coda measurements by applying empirical Green's function analysis followed by ties to independently determined moments, allowing comparison of scaling behavior worldwide. Recently, Mayeda (2003) extended these coda measurement techniques from local to regional scales by employing models of coda shape that contain up to six parameters to describe distance effects. The limited number of parameters will smooth through some coda shape variations over broad areas. We mitigate this limitation by employing the typecurve method of coda analysis. The typecurve is an empirically derived coda shape that does not rely on model assumptions. Typecurves are impractical for use over broad areas, but provide high precision measurements at local distances and for regional distance data that share a common path, such as earthquake clusters and test site explosions. Typecurve results can be combined with broad area results by correcting for the offset between the typecurve and the broad area coda shape model. This correction gives a precision that remains high within event clusters, but reverts to broad area levels between or outside clusters. We apply the combined coda method to over 6,500 events in China and central Asia, generating typecurve coda shapes for Semipalatinsk and Lop Nor explosions. The typecurve approach is especially appropriate for Borovoye archive data, as saturation forces the use of late time segments for many events, and effects of elapsed time, commonly observed for model fits to coda data, are avoided. Spectral results from this analysis are critical for studying amplitude-yield behavior for underground tests in central Asia.

OBJECTIVE

We have upgraded coda wave calibration procedures, in particular the calibration of coda shape variations, for application to Borovoye archive explosion data. This is achieved using a typecurve technique (e.g. Hartse *et al.*, 1995) that delivers extremely precise relative amplitudes for clustered events. These results can be used to constrain relationships between coda source factors and yield.

RESEARCH ACCOMPLISHED

Background material for this study has been published elsewhere, but will be repeated here for purposes of completeness. The stability of coda waves has been well established through observations that have shown coda amplitudes to be independent of distance, path details and azimuth with respect to the focal mechanism (Aki, 1969). This behavior is consistent with the generation of coda by scattering and allows accurate measurement of relative amplitudes for use in source scaling (e.g. Aki and Chouet, 1975) or site effect (Phillips and Aki, 1986) studies. Furthermore, coda amplitudes can be measured to high precision because of the redundant information in adjacent time windows. This makes coda ideal for monitoring small, sparsely recorded events for purposes of discrimination (Hartse *et al.*, 1995) and magnitude or yield estimation (Rautian *et al.*, 1979; Mayeda, 1993) as the measurement stability is equivalent to that available from a multi-station network.

The methods developed by Mayeda *et al.* (2003) are applied to obtain regional coda calibration parameters for China and central Asia stations. Records were processed from underground nuclear tests, chemical explosions and earthquakes recorded across China and central Asia (Figure 1) for purposes of calibrating coda wave behavior. Including duplicate and surrogate stations in the list, these are: AAK, BJI, BJT, BRV, BRVK, CHTO, ENH, HIA, KMI, KKAR, KK31 KUR, KURK, LSA, LZH, MAK, MAKZ, MKAR, MK31, MDJ, NIL, NVS, PDY, QIZ, SSE, TKM2, TLG, TLY, ULHL, ULN, WMQ, WUS, XAN and ZAL, as well as Borovoye archive STsR-TSG instruments KS, KSM and KSVM (Richards *et al.*, 1992; Kim and Ekstrom, 1996) and PASSCAL Tibetan Plateau Experiment stations AMDO, BUDO, ERDO, GANZ, LHSA, MAQI, SANG, TUNL, USHU, WNDO and XIGA (Owen *et al.*, 1993).

Following instrument correction, data were reduced by band-passing in 13 bands, from 0.03-0.05 to 6.0-8.0 Hz, followed by Hilbert transform envelope and smoothing operations. Final envelopes were formed by averaging the two horizontal component envelopes. Exceptions are the vertical components at short-period arrays and Borovoye archive KSVM. MKAR and KKAR array envelopes were stacked without shifting, which reduced the scatter that typically rides on top of the envelope, allowing better detection of low signal-to-noise (SNR) coda, especially in the higher frequency bands.

Coda analysis windows were determined by manual inspection for a subset of the China and central Asia envelope data that included all BRV(K), KKAR, MAK(Z), MKAR, NIL (BH), ULN, WMQ and Tibet Experiment records, all explosions, both nuclear and chemical, as well as all records of 44 earthquakes for which independently derived moments exist. The remaining data were analyzed using an automatic procedure to identify the coda window.

After manual review, we calibrated coda peak and shape parameters following the regional calibration procedure of Mayeda *et al*. (2003). First, coda peaks were determined by inspection of WMQ and NIL (BH) envelope data. In many cases, especially for low *Q* paths and high frequencies, peaks did not stand out; however a break in slope could be identified near the predicted Lg arrival. In some low *Q* path cases, the peak envelope occurred near the Sn arrival and no peak or break in slope could be identified near the Lg. Sn peaks were more commonly observed at NIL than at WMQ. Sn coda were used in the analysis if signal-to-noise were sufficient following the predicted Lg peak. The group velocities of the envelope peaks were calibrated by fitting (L_1) a flat Lg velocity along with a hyperbola with three adjustable parameters to describe the Sn velocity as a function of distance:

$$\mathbf{v_g} = \mathbf{v}_0 - \frac{\mathbf{v}_1}{\mathbf{v}_2 + \Delta}$$

where v_g is group velocity of the peak; v_0, v_1 and v_2 are adjustable parameters and Δ is distance in kilometers. Within scatter, Sn and Lg group velocities were the same for WMQ and NIL, so we applied the these calibration curves to all stations.

Coda shape was obtained by fitting the coda decay using:

$$\mathbf{a(t)} = \mathbf{a_0} \cdot \mathbf{t}^{-\alpha} \cdot \mathbf{e}^{\beta \cdot \mathbf{t}}$$

where *a(t)* is coda amplitude, *t* is time from the coda peak (taken as the smaller of the Lg and Sn velocities, see above), a_0 is the coda source factor, α is a spreading factor, and β is the coda decay parameter. The spreading factor and a distance dependent decay parameter were then fit to envelope data using direct search techniques in an L1 sense. The distance dependence of the decay parameter is described by fitted hyperbola parameters b_0, b_1 and b_2:

$$\beta = \mathbf{b}_0 - \frac{\mathbf{b}_1}{\mathbf{b}_2 + \Delta}$$

The coda shape parameters were determined for various station groups. Well sampled stations, such as WMQ, were calibrated alone. Closely located stations, such as MAK, MAKZ, MKAR and MK31, or Kirgiz network stations, were grouped together. Poorly sampled stations were grouped by regional propagation characteristics (based on two-dimensional (2D) amplitude tomography results, described below).

This coda shape method relies on four free parameters (spreading and the three hyperbola parameters that combine to represent the distance dependence of the decay parameter). The spreading can also be represented in hyperbola form, which gives six fit parameters. Even with six free parameters, we cannot expect to represent all the variations in regional coda shape. In particular, coda shape has been observed to vary laterally, and we can expect to see azimuthally dependent coda shapes in geologically heterogeneous regions. Furthermore, careful observation of coda shapes shows that various phases arrive in different bands at different times following the dominant phase in each band (see Rautian *et al.*, these proceedings). Thus, coda decay is not always uniform and ripple behavior can be superposed on an otherwise monotonically decreasing envelope. Finally, we wish to include Borovoye archive data in our study because of the rich collection of explosions recorded there. These data are often saturated and the coda measurement windows can start very late in the seismogram. Our procedures, based on using modern digital data, restrict coda windows to the early coda in order to calibrate portions of the coda that would be observable for small events. This procedure is incompatible with the Borovoye data as the early coda is often off scale. We can apply one model over the entire time interval, but this is known to be poor practice as the coda decay rates always decrease with time, due to multiple scattering or increased sampling of high *Q* materials at depth and this effect will not be captured by our parameterization.

Our solution to the coda shape problem outlined above is to use typecurve analysis (Hartse *et al.*, 1995). This technique is a variation on early coda techniques described by Aki (1969), and the common shape technique of Phillips and Aki (1986). These techniques were used to analyze local earthquake coda, where coda shapes could be expected to be similar for a wide range of event locations as long as the late coda was used, defined to start at twice the direct wave arrival time. Because we include early coda in regional work, we can only assume coda shapes similar if events are closely located relative to the path length. This holds for test site events recorded at regional distances, as well as for naturally occurring clusters of earthquakes. Assuming a constant shape for such coda envelopes, we invert for that shape without reference to a restrictive model by defining the model parameters to be the coda amplitudes over the entire range of times that are continuously sampled by the records. Typecurve results for Borovoye archive recordings of Semipalatinsk events are shown in Figure 2.

Of course, the typecurve offset is not resolvable and is set such that the mean is zero. Relative coda amplitudes are then measured by directly comparing with the typecurve, accounting for time varying error on the typecurve model terms in the calculation. This can be repeated for other stations for the same event cluster. The typecurve amplitudes are then made compatible with amplitudes measured using the four-parameter model fits, by fitting the typecurve with the appropriate shape model, and using the difference to adjust for the effect of the arbitrary typecurve level. In this way, the high precision of the typecurve measurement within clusters of events is retained, and fall back to the lower precision of the model fits over broad areas, analogous to advantages of the cross-correlation traveltime methods used in relative earthquake location. Clearly, the high precision, the lack of reliance on restrictive models and the ability to overcome problems with saturated Borovoye archive records of a large number of Soviet underground tests will greatly advance our ability to constrain amplitude-yield models for use in explosion monitoring.

We obtain raw coda source factors, a_0,using the calibrated envelope peak group velocity and coda shape factors, or the typecurve method described above. These values must be corrected for path and site effects. One-dimensional (1D) and 2D methods were used to do this. The 1D method follows Mayeda *et al*. (2003). We obtain initial path terms using a rough source correction based on mb (Taylor and Hartse, 1998) and fit (L_1) a spreading-attenuation model:

$$\mathbf{a}(\Delta) = \mathbf{s}_0 \cdot \Delta^{-\alpha} \cdot \mathbf{e}^{\frac{-\pi \mathbf{f} \Delta}{\mathbf{Q c}}}$$

where *a* is mb-corrected amplitude, s_0 represents the site effect, but contains other effects such as coda generation (media scattering strength), α is spreading, *f* is frequency, *Q* is the quality factor and *v* is velocity, to which we assign the nominal Lg velocity of 3.5 km/s. Spreading is set based on mb-corrected coda amplitudes at distances under 100 km. These values are zero at low frequencies and increase (0.7 for the 6 - 8 Hz band) with frequency. These values reflect the shrinking range over which coda amplitude is observed to be independent of distance as frequency increases. Site and *Q* terms are varied to obtain the best fit. While appearing physical, this equation is only used for empirical fitting and fit parameters must not be overinterpreted. These site and *Q* values are used as the starting point for a second refinement step.

The site and *Q* terms are further refined using data only from events recorded at more than one station. This is done by adjusting the site and *Q* models simultaneously for all stations in order to fit station-to-station amplitude ratios. This removes the influence of a possibly biased mb, which was used in the initial step to remove source effects (Mayeda *et al.*, 2003). This procedure was implemented using an L_1 criterion with direct search techniques (Press *et al.*, 2001). We note that the heterogeneous seismicity pattern results in sampling over limited distance ranges for many stations, which makes extrapolation risky using the 1D results.

Our preferred path correction method employs tomography techniques to invert for a laterally varying (2D) *Q* and relative site terms (Phillips *et al.*, 2000; Phillips *et al.*, 2001; Phillips and Hartse, 2002). The inversion equations are the same as for the 1D case above, with the addition of a sum over discretized path terms in place of 1/*Q*. Only data from multiple recorded events, similar to the second, 1D path step, is used in order to eliminate source effects by fitting station-to-station amplitude ratios. We remove a small number of outliers (less than 1% of the data) based on the 1D results and use L_2 techniques in the inversion. Spreading is set as in the 1D calculations. Currently, the tomography treats the coda as a direct path, rather than an ellipsoidal area. This is most appropriate for short codas, and misfits are low as the root mean square (RMS) residuals fall below 0.1 log10 amplitude units for all bands. For data from 2,250 multiple recorded events in the band 0.7 to 1 Hz, for example, residual variance is reduced 86% relative to the best fit, uniform *Q* model. *Q* results follow regional geology well. We are confident to extrapolate path corrections into aseismic, but well resolved areas because of the more physical nature of the tomography model.

The 2D path correction technique was applied to Berkeley Seismic Stations data that had been analyzed by Lawrence Livermore National Laboratory (LLNL) scientists using a 1D model, and a comparison of the results can be found in Mayeda *et al.*, in these proceedings.

The final calibration steps adjust measurements between bands and shift to absolute units based on independently determined moments. Adjustments between bands are calculated in order to flatten the earthquake spectra below their corners. Corner frequencies are estimated using scaling based on mb (Taylor and Hartse, 1998). We start with earthquake data from bands less than 1/4 of the corner frequency in an L_1 simplex inversion to obtain the band corrections. For our data set, this gives corrections for bands below 1 Hz. We assume an ω^2 model and allow data less than 1/2 the corner, and so on, to obtain corrections for the higher bands, which are spliced to the low frequency results. This approach was suggested by results of synthetic tests that showed that high frequency spectra can drift high by 0.1 to 0.2 $\log_{10}$ units, likely due to a slight curvature of earthquake spectra when using a liberal corner frequency cut-off.

We are fortunate to have data from 44 earthquakes for which moments have been independently determined using waveform matching techniques (Zhu *et al.*, 1997; Patton, 1998; Ghose *et al.*, 1998). An overall shift is obtained such that spectral data from bands less than 1/4 of the corner frequency, calculated as above, match the appropriate moment in a median sense. Spectra then carry units of Newton-meter (N-m). Earthquake results become moment rate

spectra and we refer to explosion results as “apparent coda source spectra” the term “apparent” indicating possible near source effects, including near source path, on the spectra.

After correction, the scatter between coda and independently derived moments is 0.18 $\log_{10}$ units. We do not use the Harvard Centroid Moment Tensor (CMT) solutions in this step because of bias due to unaccounted for crustal thickness in this area (Patton, 1998). Additional independent moments will be needed in the future to further validate our results. A broad geographical distribution would help validate the broad area path calibration. Moments for small events, perhaps obtained by applying spectral techniques to local network data, would help validate the results in higher bands.

Apparent source spectra for a well recorded Lop Nor nuclear event show good correspondence between stations (Figure 3). These spectra match especially well in the higher bands. Low frequency coda are less well studied, but direct waves are known to exhibit multipathing effects in these bands (Patton *et al.*, 1985).

The earthquake results can be summarized by fitting a two-parameter ω^2 source model. Mw and stress drop using standard formulae are calculated. Stress drop for the highest quality network spectral fits show striking regional variation in China and central Asia (Figure 4). The patterns include low stress drop events (0.1 MPa) in areas of north-central Tibet and the North China Basin. A marked gradient in stress drop can be seen starting at the Tarim Basin-Tien Shan boundary where stress drops are uniformly about 1 MPa, then moving north into the Tien Shan where stress drops increase to above 10 MPa and finally approach 100 MPa. The stress drop patterns tend to be similar from station to station. Furthermore, for station WMQ and others, the low stress Tibet events lie along similar paths as more distant, higher stress events. This indicates unaccounted for path effects are not the cause of the variations. Such variations in scaling could be included in amplitude calibration efforts for event identification (MDAC) work. We use these regional patterns to limit the events used in the spectral flattening correction to the high stress drop regions. The stress drops can also be used to constrain spectral fits and Mw in cases when the frequency band is not well sampled due to signal-to-noise or other effects.

CONCLUSIONS AND RECOMMENDATIONS

Typecurve analysis provides high precision measures of relative amplitudes of clustered events, including test site explosions. This method allowed the inclusion of saturated explosion data from Borovoye archive records, which greatly enhances our ability to calibrate coda source factors with respect to yield. We plan to further enhance our collection of central Asia, regional explosion data with pre-digital era, multispectral (ChISS) measurements, as described in Rautian et al., these proceedings.

Broad area calibration using tomographic imaging for path and site effects allows coda spectra to be displayed on a common basis throughout China and central Asia, for both earthquakes and explosions. Residuals from the tomographic inversions are remarkably low, on the order of 0.1 $\log_{10}$ units, demonstrating the internal consistency and precision of the amplitude data. Similar, two-dimensional patterns should be investigated in other coda calibration steps, including the group velocity of the peak envelope and coda shape effects.

Following 2D path corrections, the coda results show interesting scaling for earthquake sources. Earthquakes show systematic, regional variations in scaling through stress drop patterns, which could be included in event identification work (MDAC) to reduce scatter in earthquake populations of discriminants. Kriged stress drop maps have been implemented in coda calibration procedures, where emphasis on high stress drop events is useful in obtaining spectral flattening corrections and knowledge of the stress drop provides a useful constraint in fitting narrow band spectra to obtain Mw.

REFERENCES

Aki, K. (1969), Analysis of the seismic coda of local earthquakes as scattered waves, J. Geophys. Res., 74, 615-631.

Aki, K. and B. Chouet (1975), Origin of coda waves: attenuation, and scattering effects. J.Geophys.Res. 80, 3322-3342.

Ghose, S., M.W. Hamburger and C.J. Ammon (1998), Source parameters of moderate sized earthquakes in the Tien Shan, central Asia from regional moment tensor inversion, Geophys. Res. Lett., 25, 3181-3184.

Hartse, H.E., W.S. Phillips, M.C. Fehler and L.S. House (1995), Single-station spectral discrimination using coda waves, Bull. Seism. Soc. Am., 85, 1464-1474.

Kim, W-Y. and G. Ekstrom (1996), Instruments responses of digital seismographs at Borovoye, Kazakhstan, by inversion of transient calibration pulses. Bull. Seism. Soc. Am. 86, 191-203.

Mayeda, K.M. (1993), mb (Lg Coda): A stable single station estimator of magnitude, Bull. Seism. Soc. Am., 83, 851-861.

Mayeda, K.M., W.R. Walter (1996), Moment, energy, stress drop and source spectra of western United States earthquakes from regional coda envelopes, J. Geophys. Res., 101, 11195-11208.

Mayeda, K.M., A. Hofstetter, J.L. O'Boyle, W.R. Walter (2003), Stable and transportable regional magnitudes based on coda-derived moment-rate spectra, Bull. Seism. Soc. Am., 93, 224-239.

Owens, T.J., G.E. Randall, F.T. Wu and R. Zeng (1993), PASCAL instrument performance during the Tibetan Plateau Passive Seismic Experiment, Bull. Seism. Soc. Am., 83, 1959-1970.

Patton, H.J., S.R. Taylor, D.B. Harris and J.M. Mills (1985), The utility of regional Chinese seismograms for source and path studies in central Asia, Geophys. J. Royal Astr. Soc., 81, 469-478.

Patton, H.J. (1998), Bias in the centroid moment tensor for central Asian earthquakes: Evidence from regional surface wave data, J. Geophys. Res., 103, 26963-26974.

Phillips, W.S. and K. Aki (1986), Site amplification of coda waves from local earthquakes in central California, Bull. Seism. Soc. Am., 76, 627-648.

Phillips, W.S., H.E. Hartse, S.R. Taylor and G.E. Randall (2000), 1 Hz Lg Q tomography in central Asia, Geophys. Res. Lett., 27, 3425-3428.

Phillips, W.S., H.E. Hartse, S.R. Taylor, A.A. Velasco and G.E. Randall (2001), Application of regional phase amplitude tomography to seismic verification, Pure Appl. Geophys., 158, 1189-1206.

Phillips, W.S. and H.E. Hartse (2002), Regional path calibration using multiple station amplitude tomography, Seism. Res. Lett., 73, 228.

Press, W.H., S.A. Teukolsky, W.T. Vetterling and B.P. Flannery (2001), Numerical Recipes in Fortran 77: The Art of Scientific Computing, Cambridge University Press, Cambridge, U.K.

Rautian, T.G., V.I. Khalturin, I.S. Shengelia, (1979), The coda envelopes and the determination of the magnitudes of Caucasus earthquakes, The Physics of the Earth, Acad. Sci. USSR, N6 22-29 (English translation of Russian original).

Richards, P.G., W.Y. Kim and G. Ekstrom (1992), The Borovoye Geophysical Observatory, Kazakhstan, EOS, 73, 201-206.

Taylor, S.R. and H.E. Hartse (1998), A procedure for estimation of source and propagation amplitude corrections for regional seismic discriminants, J. Geophys. Res., 103, 2781-2789.

Zhu, L.P. , D. Helmberger, C.K. Saikia, B.B. Woods (1997), Regional waveform calibration in the Pamir-Hindu Kush region, J. Geophys. Res. 102, 22799-22813.

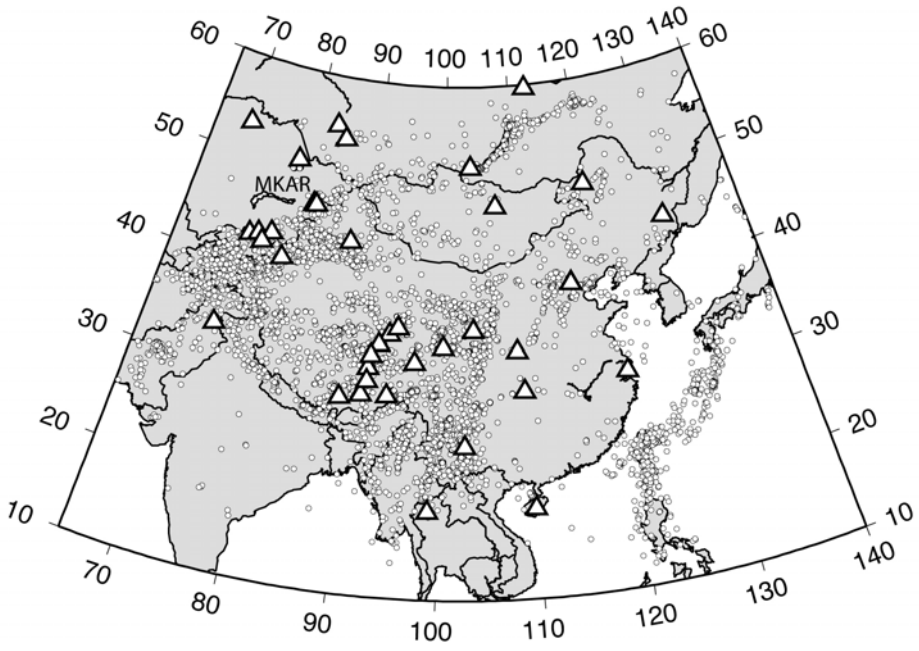

Figure 1. **Stations and events used in the coda wave study.**

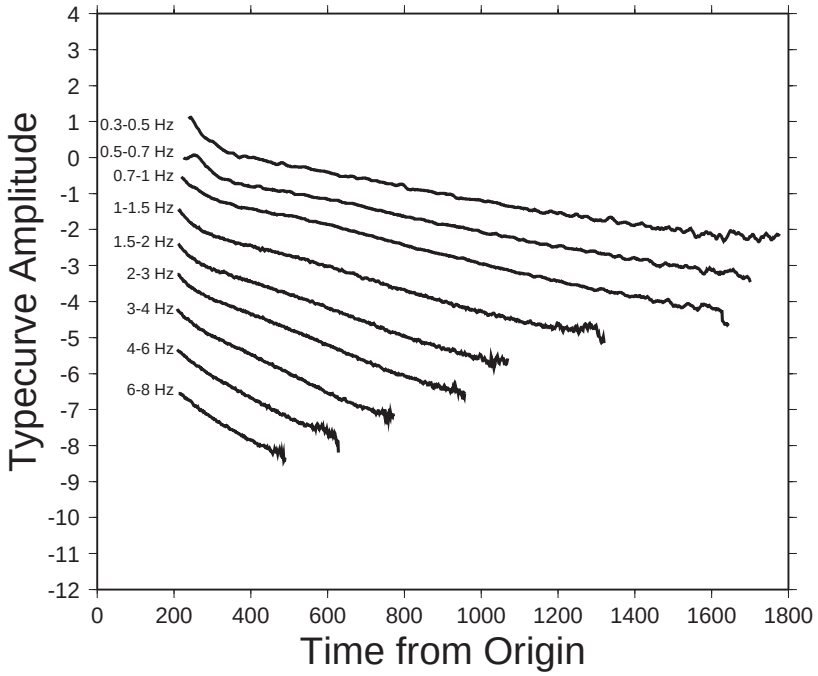

Figure 2. **Typecurves for Semipalatinsk explosions from the Borovoye archive. Balapan and Degelen results are nearly identical and all sub-areas of the Semipalatinsk test site are have been included together in these results. Typecurve levels have been shifted for plotting purposes.**

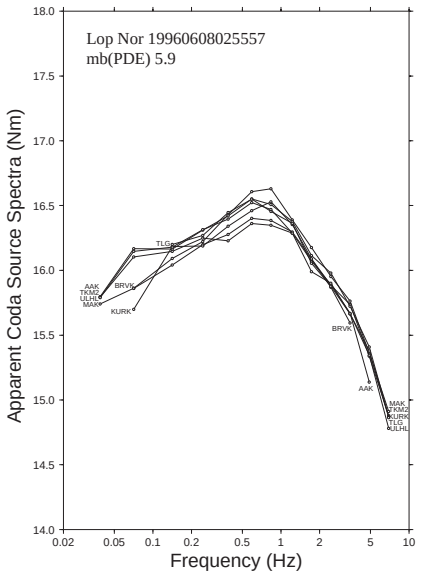

Figure 3. Apparent source spectra determined using coda wave data from seven stations for a Lop Nor test. Stations are indicated as spectra endpoints. The inter-station consistency is especially good for bands above 1 Hz.

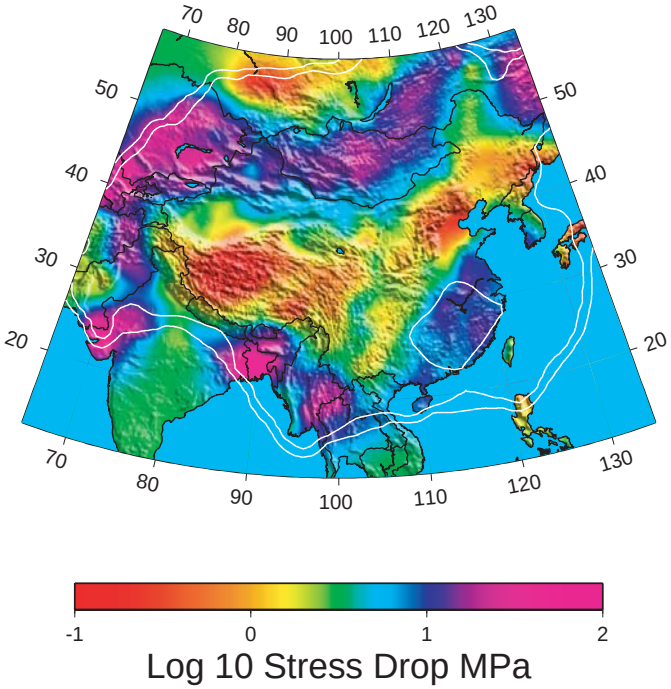

Figure 4. Kriged stress drop and error contours based on network fits of coda spectra to standard, omega-squared source model formulae. Events were restricted by requiring spectral coverage on both sides of the fitted corner frequency